Near-UV Circular Dichroism and UV Resonance Raman Spectra of Tryptophan Residues as a Structural Marker of Proteins

ARTICLE *in* THE JOURNAL OF PHYSICAL CHEMISTRY B · JULY 2013

Impact Factor: 3.3 · DOI: 10.1021/jp404685x · Source: PubMed

4 AUTHORS, INCLUDING:

Masako Nagai
Hosei University
69 PUBLICATIONS **874** CITATIONS

SEE PROFILE

THE JOURNAL OF PHYSICAL CHEMISTRY B

Article

pubs.acs.org/JPCB

Near-UV Circular Dichroism and UV Resonance Raman Spectra of Tryptophan Residues as a Structural Marker of Proteins

Shigenori Nagatomo,*[,†] Masako Nagai,[‡] Takashi Ogura,[§] and Teizo Kitagawa*[,§]

[†]Department of Chemistry, University of Tsukuba, Tsukuba, Ibaraki 305-8571, Japan

[‡]Research Center for Micro-Nano Technology, Hosei University, Koganei, Tokyo 184-0003, Japan

[§]Picobiology Institute, Graduate School of Life Science, University of Hyogo, 3-2-1, Kouto, Kamigori, Ako-gun, Hyogo 678-1297, Japan

Supporting Information

ABSTRACT: Near-UV circular dichroism (CD) and UV resonance Raman (UVRR) spectra of L-tryptophan (Trp), its derivatives, and indole-C_3 derivatives were investigated to utilize Trp signals of proteins as a structural marker. CD spectra of Trp are classified into four types: Free L-Trp gives type II (around 270 nm, L_a transition), while L-Trp in proteins generally yields type I (around 280−290 nm, L_b transition) often with vibronic structures. All the indole-C_3 derivatives except for L-Trp gave no CD bands for L_a and L_b transitions, indicating that the asymmetric carbon (C_α) connected through C_3−C_β is essential to appearance of CD. We demonstrate here that the type of CD spectra is determined by a condition of the amino group of Trp; it was changed from type II to type I by the modification of the amino group. In contrast, the modification of the carboxyl group of L-Trp had little effects on a CD spectrum. The 229 nm excited UVRR spectra were almost the same between L-Trp and indole-C_3 derivatives. Comparison of CD and UVRR spectra of Trp residues in proteins suggested that mainly the W17 (possibly together with W16) mode contributes to the characteristic vibronic coupling of L_b transition. Both UVRR and CD spectra of L-Trp were influenced by protonation of amino and/or carboxyl groups, but those changes were distinguished from hydrogen bonding effects at N_1H of indole. It is likely that these protonations are communicated to indole through σ-bonds containing C_α and thus influence both chirality of L_a and L_b transitions and properties of the B_b excited state.

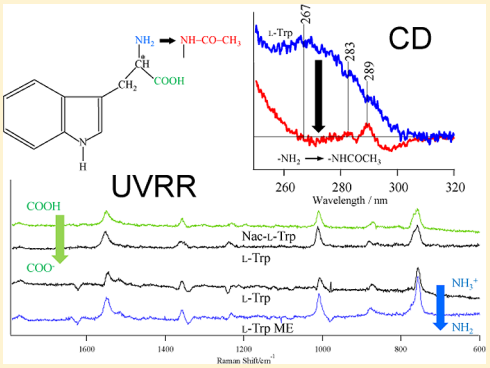

L-Tryptophan (L-Trp) is an important constituent of proteins and simultaneously can serve as a structural marker. L-Trp has four π−π^* transitions in the UV region (B_a around 195 nm, B_b around 220−240 nm, and L_a and L_b around 250−320 nm).[1] B_a and B_b are allowed degenerate transitions in benzene and therefore yield a strong band for indole, but L_a and L_b are forbidden in benzene and therefore weak for indole. L_a and L_b are energetically close but have different characters even in benzene. Thus, the near-UV absorptions of L-Trp arise from an indole side chain, and are accompanied by circular dichroism (CD). Furthermore, Raman scattering by some molecular vibrations of L-Trp are strongly intensity enhanced through resonance effects with these electronic transitions, which are known as UV resonance Raman (UVRR) spectra.[1] For instance, UVRR spectra of human adult hemoglobin (Hb A) exhibit clear changes upon the quaternary structure transition between the R (relaxed, high-oxygen affinity) and T (tense, low-oxygen affinity) states,[2−12] and also change the sign of the CD band at 287 nm.[12−16] Therefore, a correct understanding of the spectral changes of L-Trp on the basis of physical chemistry is indispensable to investigate structure−function relationships of various proteins.

According to Strickland,[17] CD spectra of Trp are classified into four types. In type I, the L_b transition gives a strong CD band, whereas the L_a transition gives little or no CD bands. Their CD spectra are dominated by two vibronic bands at 281 nm (0 + 865 cm^{-1}) and 288 nm (0−0), both of which always have the same sign, either positive or negative. In type II, the CD spectrum arises mainly from the L_a transition and lacks the vibronic structures. In type III, both L_a and L_b transitions have obvious CD bands as observed for cyclo(His-Trp). Type IV includes all which do not belong to type I, II, or III. The CD spectrum of *N*-acetyl-L-Trp ethylester (Nac-L-Trp EE), which is a typical model compound of L-Trp residue in proteins, gives a CD spectrum of typical type I, while isolated L-Trp and D-Trp yield a typical type II CD spectrum. However, a relation between structures or environments of Trp residues in proteins and types of CD spectra as well as vibrational modes yielding the characteristic coupling remains to be clarified.

The present study was undertaken to elucidate a type of CD spectra in terms of the structure of Trp or its environment.

Received: May 12, 2013
Revised: July 13, 2013
Published: July 17, 2013

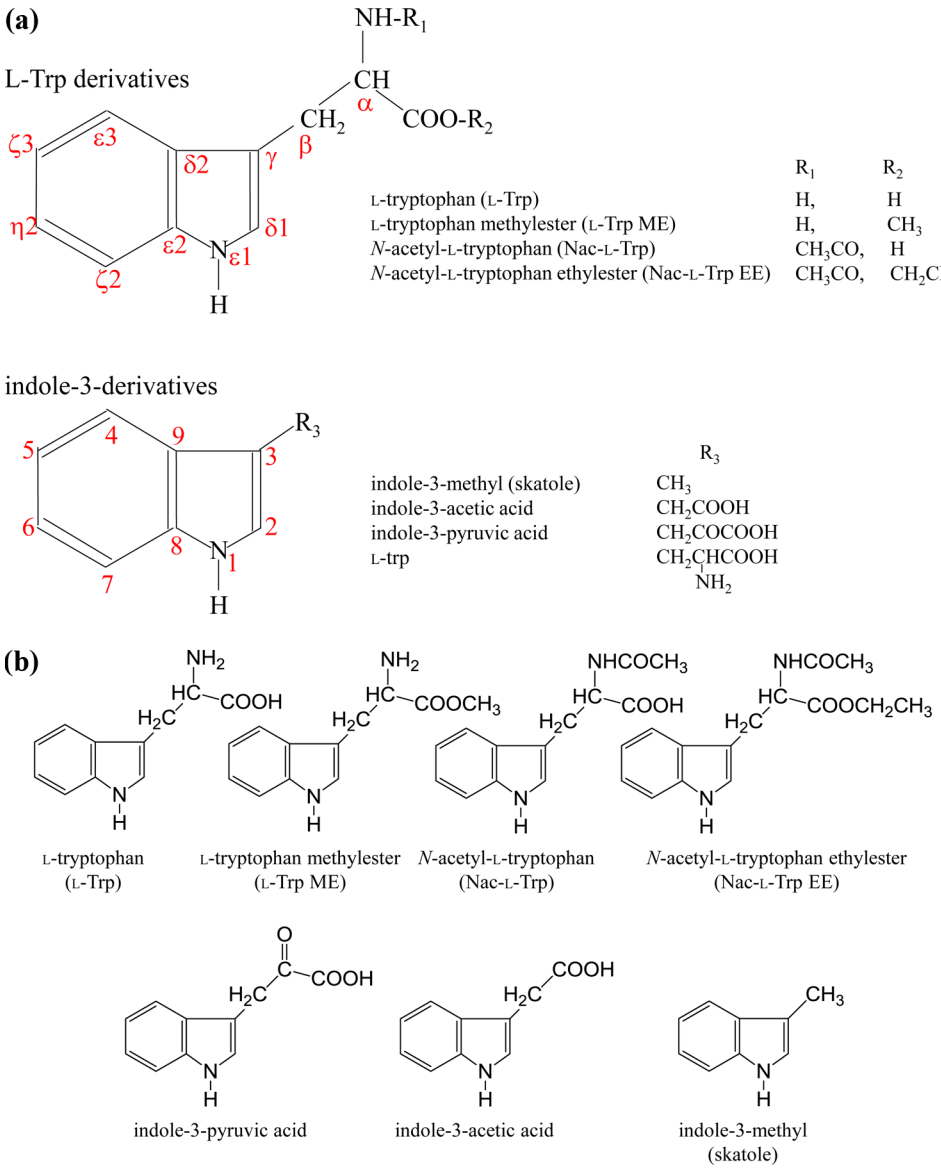

Figure 1. (a) Atomic numbering for L-Trp and indole-C_3 derivatives and abbreviations of compounds used in this study. (b) Complete chemical drawings and abbreviations of compounds used in this study.

Since Trp is an amino acid having an indole side chain through C_α−C_β−C_3 bonds and an indole itself exhibits UV absorptions but no CD, we investigated near-UV CD and UVRR spectra of various derivatives of L-Trp and C_3-substituted indole. We also try to specify vibrational modes contributing to the vibrational coupling by observing the UVRR spectra of the same samples as those used for CD measurements. The atomic numbering and structures of indole and L-Trp together with names of all the derivatives treated in this study and their abbreviations are represented in Figure 1. The results obtained from the model compounds are compared with those of specified Trp residues in Hb A extracted from the difference between Hb A and its mutants with the substitution of non-aromatic residue for a particular Trp residue.

MATERIALS AND METHODS

Reagents. L-Tryptophan (L-Trp) (Aldrich), L-tryptophan methylester (L-Trp ME) (Aldrich), *N*-acetyl-L-tryptophan (Nac-L-Trp) (Aldrich), *N*-acetyl-L-tryptophan ethylester (Nac-L-Trp EE) (Aldrich), indole-3-methyl [skatole] (Wako) and indole-3-acetic acid (Wako), and indole-3-pyruvic acid (Sigma) were used as purchased.

Hemoglobin Preparation and Purification. Hb A was purified from human hemolysate by preparative isoelectric focusing.[7] Mutant hemoglobins were prepared by a site-directed mutagenesis in *E. coli*. The Hb A expression plasmid, pHE7,[18] containing human α- and β-globin genes and the *E. coli* methionine aminopeptidase gene, was kindly provided by Professor Chien Ho of Carnegie Mellon University. Plasmids for recombinant hemoglobins (rHb's), rHb(βW15L) and rHb(βW37H), were produced using an amplification procedure for closed circular DNA *in vitro*[19] and transformed into *E. coli* JM109. *E. coli* cells harboring the plasmid were grown at 30 °C in terrific broth (TB) medium.[18] Expression of rHb was induced by adding isopropyl β-thiogalactopyranoside. The culture was then supplemented with hemin (30 μg/mL) and glucose (15 g/L), and the growth was continued for 5 h at 32 °C. The cells were harvested by centrifugation and stored under frozen conditions at −80 °C until needed for purification.

dx.doi.org/10.1021/jp404685x | J. Phys. Chem. B 2013, 117, 9343−9353

Recombinant Hb's were purified according to the methods described before.[20]

CD Measurements. The measurements were carried out with a Jasco J-820 spectropolarimeter at 25 °C using a (+)-10-camphor-sulfonic acid for calibration. Although the concentrations of all Hb samples were made the same, each observed spectrum was converted to mol CD ($\Delta\varepsilon$) and difference spectra were calculated. Absorption spectra were measured with a double-beam spectrophotometer (Hitachi, model U-3010).

UVRR Measurements. *235 nm Excitation.* UVRR spectra were excited with a XeCl excimer laser-pumped dye laser (Lambda Physik, model LPX120i and SCANMATE). The 308 nm line from the XeCl excimer laser (operated at 100 Hz) was used to excite coumarin 480, and the 470 nm output from the dye laser was frequency-doubled with a β-BaB_2O_4 crystal to generate 235 nm pulses. The Raman excitation light (3−4 mJ/cm^2) was introduced into samples at a 135° backscattering geometry from the lower front side of a spinning cell. Details of the measurement system were described previously.[21,22]

In this measurement, however, the spinning cell was moved vertically by 1 mm for every spectrum (every 5 min) to shift the laser illumination spot on the sample. The temperature of the sample solution was kept at 10 °C by flushing with cooled N_2 gas against the cell. The scattered light was collected with Cassegranian optics with f/1.1. One spectrum is composed of the sum of 400 exposures, each exposure accumulating the data for 0.8 s. All samples contained a common amount of sulfate ions, the 980 cm^{-1} band of which was used as an internal intensity standard for difference calculations of spectra.[23] Raman shifts were calibrated with cyclohexane. The integrity of the sample after exposure to the UV laser light was carefully confirmed by the visible absorption spectra measured before and after the UVRR measurements. If some spectral changes were recognized, the Raman spectra were discarded. Visible absorption spectra were recorded with a Hitachi 220S spectrophotometer.

229 nm Excitation. The excitation light at 229 nm (0.5 mW) was obtained from an intracavity frequency-doubled Ar^+ ion laser (Coherent, Innova 300C FRED), and the sample was contained in a quartz NMR tube (Wilmad-LabGlass, 535-PP-9SUP, diameter = 5 mm), which was spun using a hollow axis motor (Oriental Motor, BLU220A-5FR) at 160 rpm.[12] The measurement system used is composed of the prefilter-coupled 1 m single spectrograph (HORIBA Jobin Yvon, 1000M) equipped with a 200 nm blazed holographic grating with 3600 grooves/mm and a liquid-nitrogen-cooled UV-coated CCD detector (Roper Scientific, Spec10:400B/LN).[7,9] Each spectrum is the sum of 60 exposures, each exposure accumulating data for 30 s. Raman shifts were calibrated with cyclohexane as a frequency standard, and the frequency accuracy was ±1 cm^{-1} for well-defined Raman bands. Other procedures are common to those for 235 nm excitation.

RESULTS

Changes of near-UV CD and UVRR Spectra of Two Trp Residues in Hb A upon Quaternary Structure Transition. To clarify the problems raised by this study, we first illustrate what should be interpreted by using model compounds in terms of the structure or environment of Trp residues. Figure 2 shows CD spectra of β15Trp (A) and β37Trp (B) residues of Hb A in the T (deoxy) and R (oxy) quaternary states and the T-minus-R difference of individual Trp. Spectra for β15Trp and β37Trp were digitally obtained from the differences between

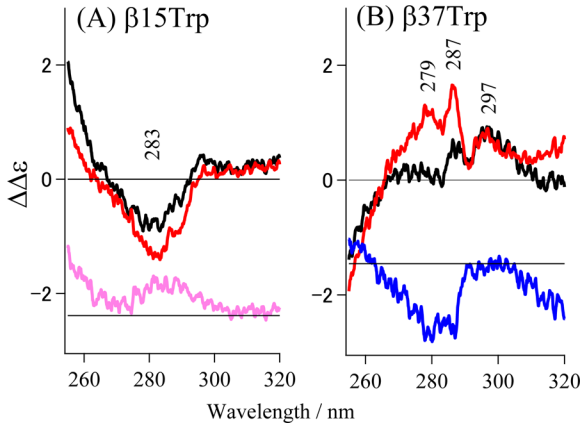

Figure 2. CD spectra of β15Trp and β37Trp residues of Hb A in the deoxy (T) and oxy (R) quaternary states and their differences. Hb, 50 μM (in heme) in a 0.05 M phosphate buffer (pH 7.0) was measured in a cell having a 2 mm light path length at 25 °C. The scan speed was 20 nm/min, and 40 scans were averaged. The spectrum for β15Trp was obtained from the difference between Hb A and rHb(βW15L), and that for β37Trp was from the difference between Hb A and rHb(βW37H) in the presence of 2 mM IHP, respectively. Red spectra, oxy-form; black spectra, deoxy-form; pink and blue spectra, difference between the deoxy- and oxy-form in β15Trp and β37Trp, respectively.

Hb A and rHb(βW15L) mutant and between Hb A and rHb(βW37H) mutant in the presence of 2 mM inositol hexaphosphate (IHP), respectively.[12] Since the concentrations of Hb A, rHb(βW15L), and rHb(βW37H) were made exactly the same, the difference spectra were obtained without an internal intensity standard in terms of mol CD ($\Delta\varepsilon$). The rHb(βW37H) mutant dissociated into dimers with low cooperativity in ordinary solvent conditions, but it was stabilized in a tetramer in the presence of IHP and exhibited significant cooperativity.[12] Although each spectrum derives from a Trp residue in an identical subunit, these spectra and also their changes upon the quaternary structure transition are distinctly different from each other. In practice, the CD spectrum for β15Trp shows a negative band at 283 nm (L_b transition) with no discernible vibronic structures and the feature does not change upon quaternary structure change, whereas that for β37Trp shows positive vibronic maxima at 279 nm (0 + 2172 cm^{-1}), 287 nm (0 + 1173 cm^{-1}), and 297 nm (0−0), and the intensities of the 0−1 and 0−2 transitions are altered by the quaternary structure change. However, on the basis of the peak positions, the CD spectra of both β15Trp and β37Trp derived from the L_b electronic transition and therefore belong to type I.

Figure 3 shows the 235 nm excited UVRR spectra of β15Trp (A) and β37Trp (B) residues of Hb A in the T (deoxy) and R (CO) quaternary states and the T-minus-R difference of individual Trp residues. Assignments of RR bands for L-Trp are based on Harada and co-workers.[24−26] Spectra of individual Trp residues were digitally obtained by subtraction of the UVRR spectrum of rHb(βW15L) or rHb(βW37H) with IHP from that of WT (Hb A). The difference spectra were calculated with the 980 cm^{-1} band of Na_2SO_4 present as an internal intensity standard. The UVRR spectra of β15Trp (A) and β37Trp (B) are rather alike in the T state except for a wavenumber of the W3 band, which is known to reflect the dihedral angle ($\chi^{2,1}$) of the $C_2-C_3-C_\beta-C_\alpha$ bonds. The dihedral angles for β15Trp and β37Trp determined with W3

dx.doi.org/10.1021/jp404685x | J. Phys. Chem. B 2013, 117, 9343−9353

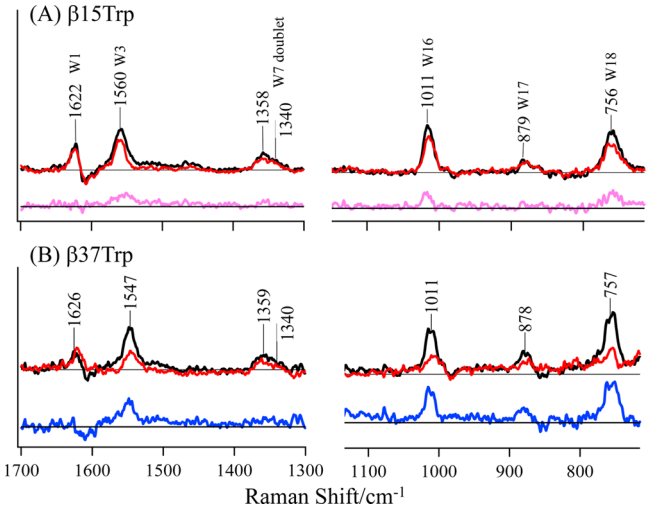

Figure 3. 235 nm excited UVRR spectra of β15Trp and β37Trp of Hb A in the deoxy (T) (black) and CO (R) (red) quaternary states, and their differences (pink and blue spectra). The spectrum of an individual Trp residue was digitally obtained by subtraction of the UVRR spectrum of rHb(βW15L) or rHb(βW37H) in the presence of 2 mM IHP from that of WT (Hb A), which contains the same amount of Na_2SO_4 as a Raman intensity standard.

frequencies are 125 and 87°, respectively.[12,26] However, the spectral changes upon quaternary structure transition are distinctly different between β15Trp and β37Trp, particularly in intensities of W16, W17, and W18 bands.

Chi and Asher pointed out that intensity increases in the 229 nm excited Raman spectra of Trp in protein result from red shifts of the $\pi-\pi^*$ absorption bands caused by environmental changes such as increased hydrogen bond donor basicity, decreased hydrogen bond acceptor acidity, and increased polarity.[27] Increase of solvent accessibility of Trp residues buried also contributes to it,[27,28] although some of the Trp bands decrease Raman intensities upon denaturation.[27,28] It is established that intensities of W16 and W18 bands reflect the hydrophobicity around the indole ring of Trp when N_1H is hydrogen bonded; the more hydrophobic surroundings, the stronger the Raman intensity is.[29] Figure 3 indicates that the environment around β37Trp is greatly changed by the quaternary structure transition, but that of β15Trp is little altered. The frequency of the W17 band reflects the strength of the hydrogen bond at N_1H, since this mode involves atomic displacements of the N_1H group, ~883 cm^{-1} for non-H-bonding and ~871 cm^{-1} for H-bonding.[25] The CD and UVRR results are consistent in the sense that the vibronic coupling is more conspicuous for β37Trp than β15Trp and that β37Trp exhibits a larger difference between the T and R quaternary structures than β15Trp. Judging from the frequency separation observed in Figure 2B, W16 and W17 are likely candidates for vibronic coupling. This will be discussed later.

CD and UVRR Spectra of *N*-Acetyl-L-Trp Ethylester (Nac-L-Trp EE). Trp residues in protein are different from an isolated Trp molecule, because they form a peptide bond at both ends. Considering the peptide bonds, we used *N*-acetyl-L-Trp ethylester (Nac-L-Trp EE) as a model of Trp residue in proteins. Nac-L-Trp EE has an amide bond ($-NHCOCH_3$) at the amino side of a Trp molecule and an ester bond ($-COOCH_2CH_3$) at the carboxyl side. Figure 4 compares absorption and CD spectra of L-Trp with those of Nac-L-Trp EE dissolved in water. Their absorption spectra are almost the

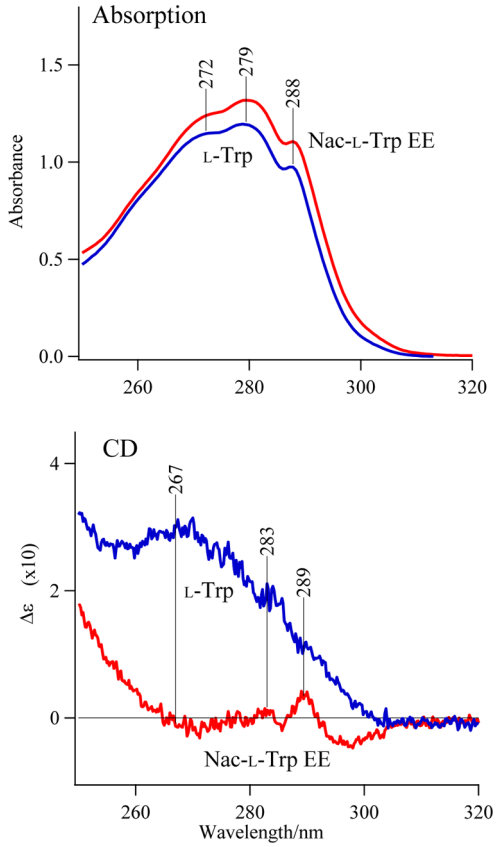

Figure 4. Absorption (top) and CD spectra (bottom) of L-Trp (blue) and Nac-L-Trp EE (red) dissolved in water.

same, giving rise to bands assignable to the L_a (272 nm) and L_b (279 and 288 nm) transitions.[30,31] The CD spectrum of L-Trp yields a large positive band at 267 nm derived from the L_a electronic transition (type II), while that of Nac-L-Trp EE gives weak positive bands with vibronic structures at 283 nm (0 + 734 cm^{-1}) and 289 nm (0−0) derived from the L_b electronic transition (type I). This indicates that modification of amino and/or carboxyl groups connecting with α-carbon (C_α) of L-Trp significantly influences the CD spectrum.

Figure 5 shows UVRR spectra of L-Trp and Nac-L-Trp EE dissolved in water. Both spectra are almost the same. Thus, CD spectra reflect features different from UVRR spectra. This suggests that the 229 nm excited UVRR spectrum is solely in resonance with the B_b transition, which depends only on the electronic state of the indole ring but is not affected by modification of amino and/or carboxyl groups of L-Trp. However, detailed spectral features are slightly different between the two compounds regarding intensity ratios of the W7 doublet and of W10 and W9. The intensity ratios of the W7 doublet, $I_{\sim1360}/I_{\sim1340}$ are 1.2 and 1.3 for L-Trp and Nac-L-Trp EE, respectively. The value for L-Trp around pH 7 is compatible with that reported previously (1.1).[24] Recently, Schlamadinger et al.[32] pointed out that the intensity ratio, I_{w10}/I_{w9}, is an unambiguous indicator for N_1-H hydrogen bonding. The I_{w10}/I_{w9} ratio estimated through deconvolutions using typical fitting analysis with two Gaussians is 4.2 for L-Trp and 2.2 for Nac-L-Trp EE. The latter value is in good agreement with the reported one (2.2).[32] The value for L-Trp is higher, and their wavenumbers themselves are also higher than those for Nac-L-Trp EE. Such differences in N_1H hydrogen bonding environment might cause the differences in their CD spectra.

dx.doi.org/10.1021/jp404685x | J. Phys. Chem. B 2013, 117, 9343−9353

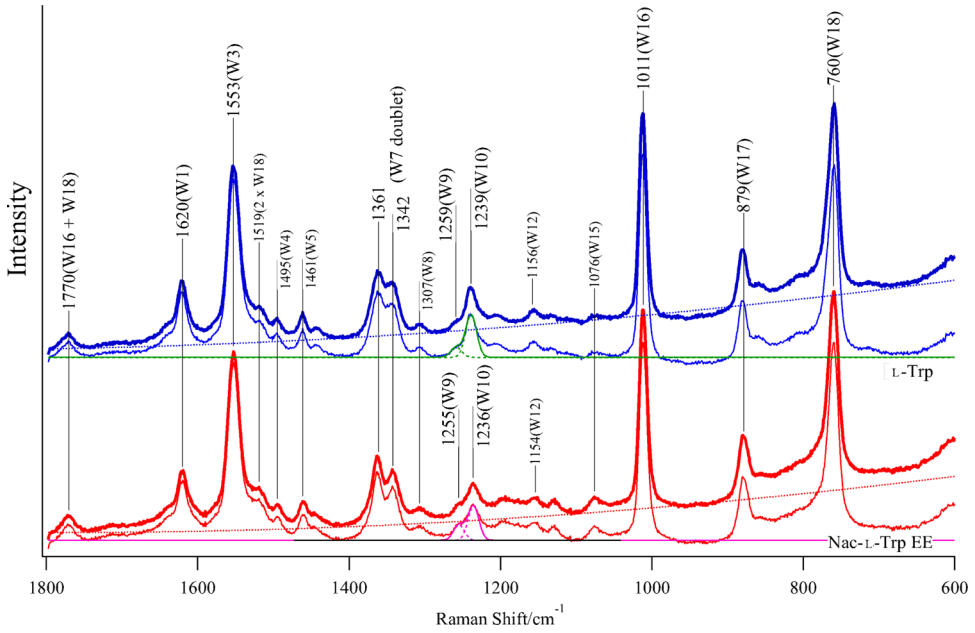

Figure 5. UVRR spectra of L-Trp (blue) and Nac-L-Trp EE (red) dissolved in water. The thin solid and broken lines indicate the spectra after baseline correction and Gaussian-fitted bands for W9 and W10, respectively.

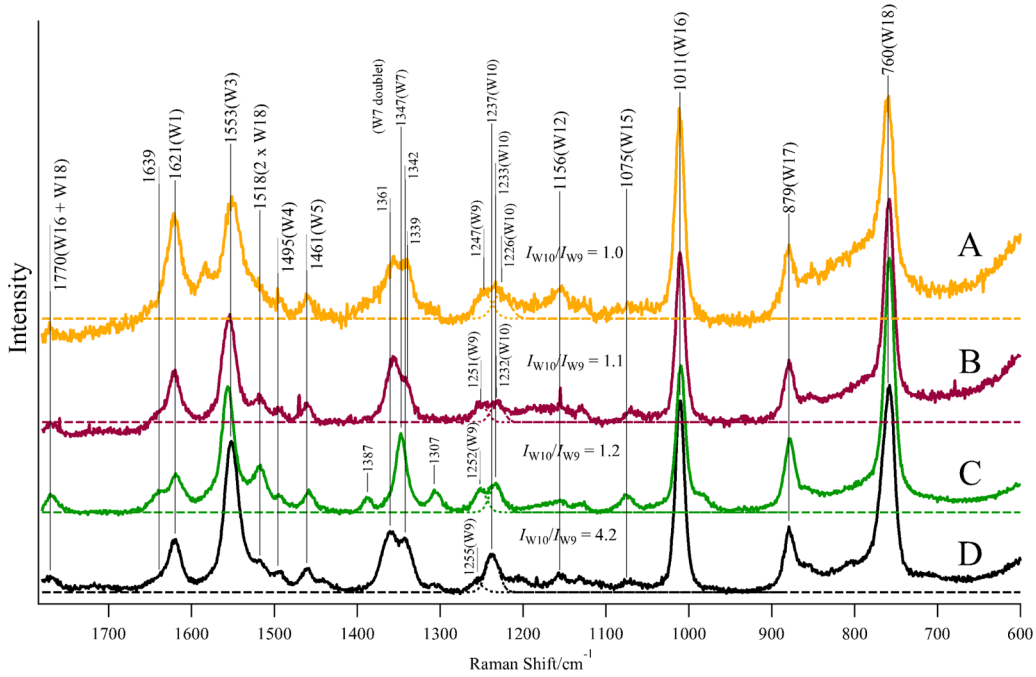

Figure 6. 229 nm excited UVRR spectra of indole-C_3 derivatives dissolved in water: indole-C_3-pyruvic acid (A), indole-C_3-acetic acid (B), indole-C_3-methyl (C), and L-Trp (D). The Gaussian-fitted bands are also represented for W9 and W10.

Influences of the C_3 Substituent of Indole Ring on CD and UVRR Spectra. Figure 6 shows the 229 nm excited UVRR spectra of L-Trp and three kinds of indole-C_3 derivatives dissolved in water. The length of the side chain is different among C_3-methyl (skatole), C_3-acetic acid, and C_3-pyruvic acid (see Figure 1). Their spectra are slightly different from those of L-Trp. The W7 band appears as a singlet for C_3-CH_3, while it is a doublet with different relative intensities in others. The intensity of W1 compared with W3 for $C_3-CH_2-CO-COOH$ is the strongest among the four spectra, while peak frequencies are alike. However, except for these minor points, the overall spectra of three indole-C_3 derivatives are very similar to that of L-Trp.

About the I_{w10}/I_{w9} intensity ratio mentioned above, L-Trp gives the largest value, while three indole-3 derivatives yield a similar value (=1.0−1.2, as shown in the figure). Schlamadinger et al. reported that the I_{w10}/I_{w9} value for skatole in 1,4-dioxane, a polar solvent, was 1.2,[32] in close agreement with the present value for water. Presumably, water serves as a hydrogen bond acceptor for indole similar to 1,4-dioxane, although their relative polarities are different and also affect Nac-L-Trp EE.[12]

Figure 7 compares CD spectra of L-Trp (black) with those of C_3-methyl (green), C_3-acetic acid (violet), and C_3-pyruvic acid

dx.doi.org/10.1021/jp404685x | J. Phys. Chem. B 2013, 117, 9343−9353

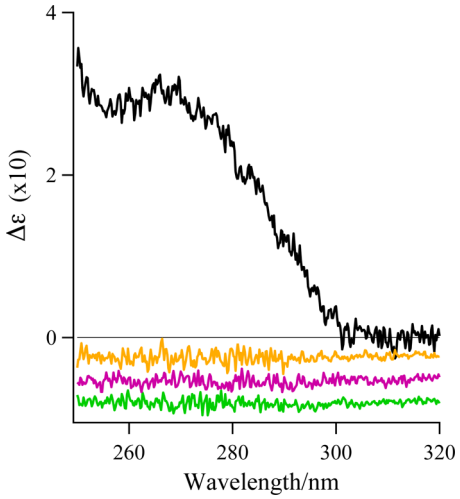

Figure 7. CD spectra of indole-C_3-methyl (green), indole-C_3-acetic acid (violet), indole-C_3-pyruvic acid (orange), and L-Trp (black) dissolved in water. All spectra are represented in the same scale, but the lower three spectra are shifted against the *y*-axis to avoid overlap of them.

(orange) derivatives of indole dissolved in water. Contrary to the results shown in Figure 6, the difference between L-Trp and three indole-C_3 derivatives is definite. Namely, all three indole derivatives exhibit no CD bands. This indicates that the existence of an asymmetric carbon (C_α) at $C_3-C_\beta-C_\alpha$ of indole is essential for the appearance of the CD spectrum of L-Trp.

Influences of the Modifications of Amino and Carboxyl Groups of L-Trp on CD and UVRR Spectra. Figure 8 compares absorption and CD spectra of *N*-acetyl-L-Trp (Nac-L-Trp) and L-Trp methylester (L-Trp ME) with those of L-Trp and Nac-L-Trp EE, all dissolved in water. Their absorption spectra are alike, but CD spectra are different. Nac-L-Trp and Nac-L-Trp EE show CD spectra of type I (L_b transition) in which vibronic CD bands are observed at 283 nm (0 + 734 cm^{-1}) and 289 nm (0−0) with the same sign and with no obvious CD intensities at 267 nm. In this case, the frequency separation is close to the frequency of W18 in Figure 5. In contrast, L-Trp ME and L-Trp show CD spectra of type II (L_a transition) lacking any major vibronic structures. These results clearly indicate that the modification of the amino group of L-Trp changes a CD spectrum from type II (L_a) to type I (L_b). It is stressed that the modification of the carboxyl group of L-Trp has little effects on a CD spectrum.

pH Dependent Changes of CD and UVRR Spectra of L-Trp Derivatives. To see the effects of protonation on CD spectra, pH dependences were examined. Figure 9 shows CD spectra of L-Trp, Nac- L-Trp, and L-Trp ME at pH 2, pH 6, and pH 12. CD spectra of L-Trp change with pH due to protonation to amino or carboxyl groups: $-NH_3^+$, −COOH at pH 2; $-NH_3^+$, $-COO^-$ at pH 6; and $-NH_2$, $-COO^-$ at pH 12. L-Trp and L-Trp ME always give positive CD bands. The former gave a similar spectrum at pH 6, and 12, reflecting the state of the carboxyl group, but the latter gave an identical spectrum at pH 2 and pH 6 ($-NH_3^+$), responding to the state of the amino group. Nac-L-Trp gave positive CD at pH 2 (−COOH) and negative ones at pH 6 and pH 12 ($-COO^-$), although the frequency separations of vibronic structures remain unaltered at 276 nm (0 + 1630 cm^{-1}), 282 nm (0 + 859 cm^{-1}), and 289 nm (0−0) in the three spectra presented. By protonation to a

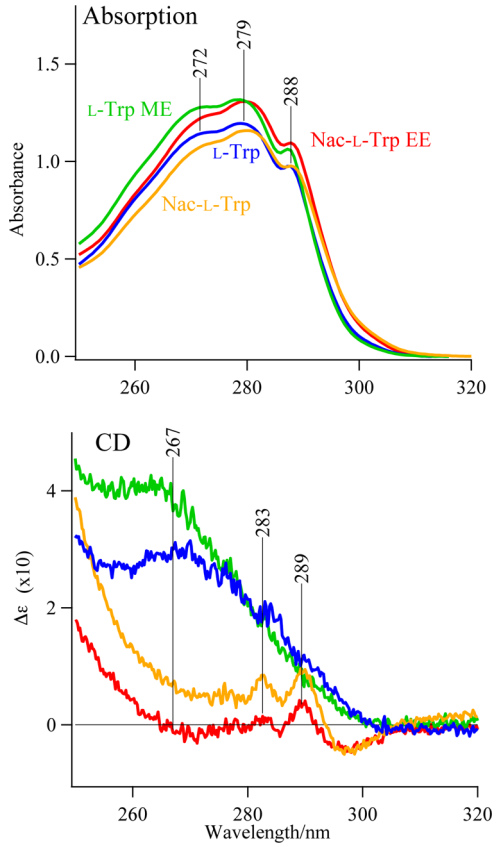

Figure 8. UV−vis absorption (top) and CD spectra (bottom) of L-Trp (blue), Nac-L-Trp (orange), L-Trp ME (green), and Nac-L-Trp EE (red) dissolved in water.

carboxyl group, common positive vibronic features of L_b are changed to negative. These results demonstrate that the effects of protonation on CD spectra are different and depend on the state of the other terminus. Therefore, some caution is required when the Trp residue is located at the N- or C-terminus of proteins, although otherwise such changes are not expected.

Figure 10 shows the raw UVRR spectrum of L-Trp (top) and the pH difference in UVRR spectra of the same samples, as shown in Figure 9. L-Trp ME reflects the UVRR spectral changes caused by protonation to the NH_2 group ($-NH_3^+$ at pH 2 and 6 and $-NH_2$ at pH 12), because the carboxyl group is esterified. Upon deprotonation of $-NH_3^+$, the higher frequency counterpart of the W7 doublet (∼1360 cm^{-1}), W3, W10, W16, W17, and W18 are intensified, whereas W1 and the lower frequency counterpart of W7 (∼1340 cm^{-1}) are weakened. For L-Trp, the effects of deprotonation of −COOH are added to those of L-Trp ME, as seen in the pH 6-minus-pH 2 difference spectrum. Its effects, however, are similar to those seen upon deprotonaton of the $-NH_3^+$ group except for W1 and the lower wavenumber component of W7. The pH dependence of the intensity ratios of W7 doublet, $I_{\sim1360}/I_{\sim1340}$, is compatible with that reported previously for L-Trp, Nac-L-Trp, and L-Trp ME.[24] The effects of deprotonation of the $-NH_3^+$ group are lacking for Nac-L-Trp, because its amino group is acetylated, while the deprotonation effects of the COOH group remain unchanged, as seen in the pH 12-minus-pH 2 and pH 6-minus-pH 2 difference spectra.

There are small differences between deprotonation of −COOH and $-NH_3^+$; upon deprotonation of $-NH_3^+$, intensities of W1 and the lower wavenumber component of

dx.doi.org/10.1021/jp404685x | J. Phys. Chem. B 2013, 117, 9343−9353

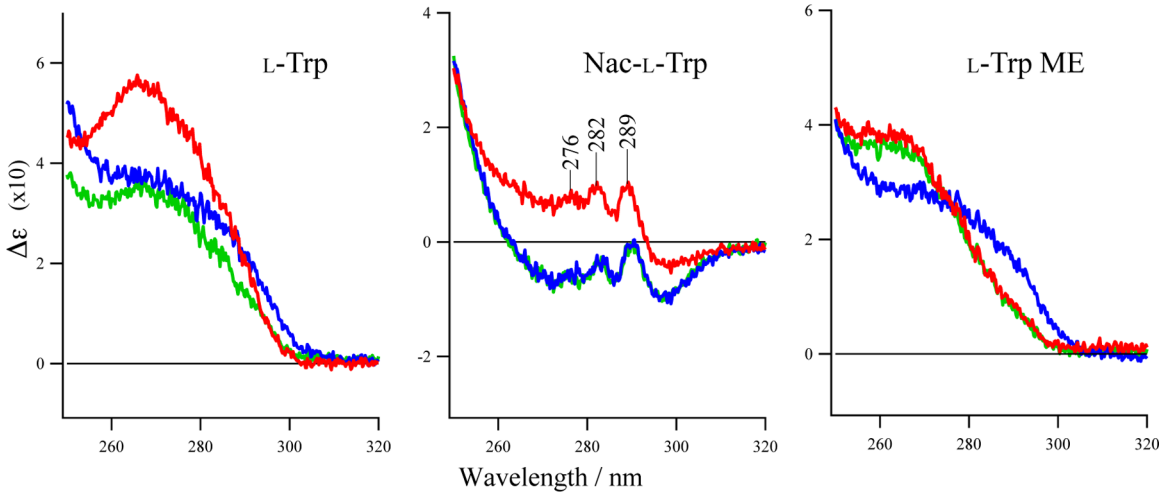

Figure 9. CD spectra of L-Trp (left), Nac-L-Trp (middle), and L-Trp ME (right) at three different pH's. Red, pH 2; green, pH 6; blue, pH 12.

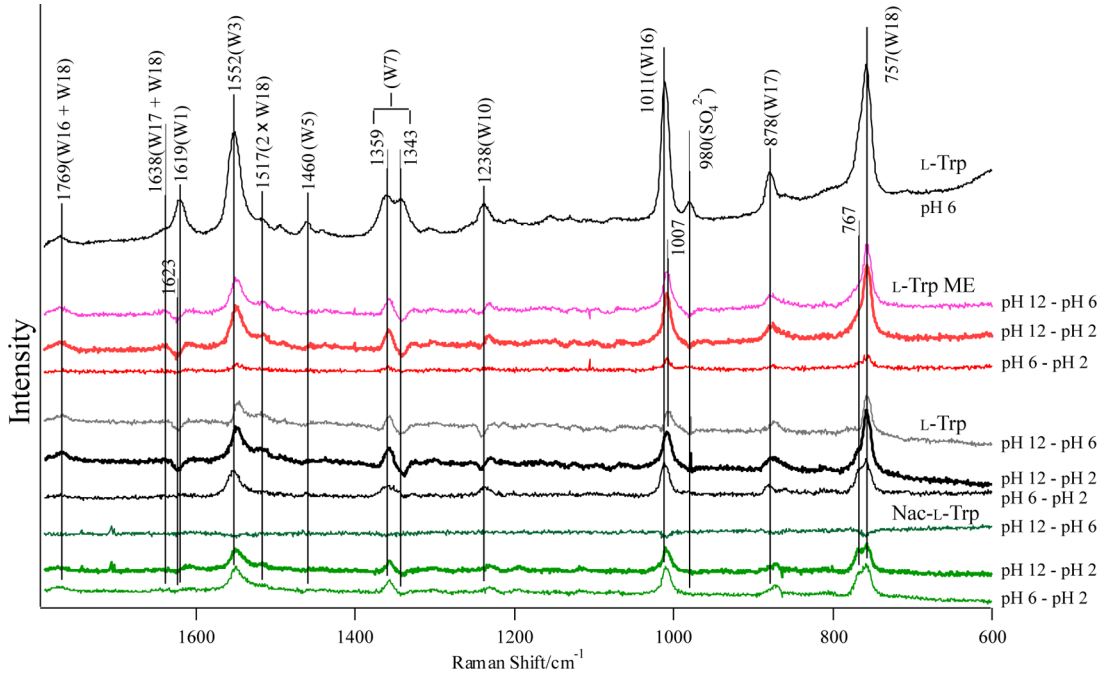

Figure 10. Raw UVRR spectrum of L-Trp (top) and pH difference UVRR spectra of L-Trp ME, L-Trp, and Nac-L-Trp.

W7 doublet (~1340 cm^{-1}) decrease. A unique feature in the UVRR of Nac-L-Trp is the appearance of an extra band at the higher frequency side (by ca. 5 cm^{-1}) of W18 upon deprotonation of −COOH. The frequency separation in the vibronic structure of L_b (0 + 859 cm^{-1}) is close to the W17 frequency. These data would be practically important when Trp is located at both ends of proteins. Here, it is stressed that the presence or absence of an electric charge affects the electronic state of the indole ring, resulting in appreciable changes of resonance enhancement of Raman intensities without changes of the vibrational frequencies of the indole ring. This may suggest a shift of the π electronic B_b band. When we compare pH dependent UVRR spectra of L-Trp, Nac-L-Trp, and L-Trp ME (Figure 10) with UVRR spectra of Nac-L-Trp EE dissolved in water (Figure 5), the effects of protonation or deprotonation of amino or carboxyl group on UVRR spectra are larger than those of acetylation or esterification of them.

Furthermore, we found a small but important difference between deprotonation effects of amino and carboxyl groups on UVRR spectra. The difference spectrum (pH 6-minus-pH 2) of Nac-L-Trp is almost the same as the difference spectrum of L-Trp, which arises from deprotonation of −COOH to $-COO^-$, independent of modification ($-NH_3^+$ or CH_3CONH-) of the N-terminus. Deprotonation from −COOH to $-COO^-$ causes small wavenumber shifts (1−2 cm^{-1}) of W10 bands from 1235 to 1233 cm^{-1} in Nac-L-Trp (Figure SI1, Supporting Information) and from 1239 to 1238 cm^{-1} in L-Trp, respectively (Figures SI2 and SI3, Supporting Information).

On the other hand, a difference spectrum (pH 12-minus-pH 6) of L-Trp ME is different from the corresponding difference spectrum of L-Trp, which arises from deprotonation of $-NH_3^+$ to $-NH_2$. The W10 bands of both L-Trp ME and L-Trp exhibit a shift to low wavenumbers upon deprotonation of $-NH_3^+$, but its intensity increases for L-Trp ME whereas decreases for L-Trp. This suggests that modification of the C-terminus

dx.doi.org/10.1021/jp404685x | J. Phys. Chem. B 2013, 117, 9343−9353

($-COO^-$ or $-COOCH_3$) influences the intensities of W10 bands. Deprotonation from $-NH_3^+$ to $-NH_2$ causes relatively large wavenumber shifts (3−5 cm^{-1}) of W10 bands from 1238 to 1235 cm^{-1} in L-Trp ME (Figure SI4, Supporting Information) and from 1238 to 1233 cm^{-1} in L-Trp (Figures SI2 and SI3, Supporting Information).

DISCUSSION

Basic Properties of Electronic Transitions of L-Trp and Indole and CD Spectra. Electronic transitions of the indole ring were treated theoretically by Albinsson and Norden,[33] who demonstrated that the transition dipoles of B_b, L_a, and L_b absorptions of L-Trp dissolved in water are as illustrated in Figure SI5 in the Supporting Information. A sharp absorption band at 218 nm is ascribed to the B_b transition, while the weak bands at 270 and 287 nm are assigned to the L_a and L_b transitions, respectively, whose transition moments are approximately orthogonal.[34] Near-UV tryptophanyl CD bands become complicated due to extensive overlapping of the L_a and L_b transitions. Both transitions are dipole inactive in benzene and have different properties but become active due to attachment of a pyrrole ring to benzene. Therefore, absorption intensities for L_a and L_b are much weaker than that of the B_b transition which is allowed in benzene. For an indole derivative, L_b is characterized by the presence of vibronic structures, that is, 0−0 and 0−1 (0 + 850 cm^{-1}).[35] This feature is also retained by L-Trp and its derivatives, although the frequency separations in the vibronic coupling are not always determined precisely for proteins. It is noted, however, the frequency separations in all the Trp residues and their model compounds examined in this study are distributed in the 1200−730 cm^{-1} range. Although the observed frequency separations indicate the vibrational frequencies in the electronic excited state, we discuss it on the basis of those in the ground electronic state as the first approximation.

In the frequency region between 1200 and 730 cm^{-1}, there are only three in-plane vibrational modes—W16, 1011 cm^{-1}; W17, 879 cm^{-1}; W18, 756 cm^{-1}—in Figure 3. For the W16 and W18 modes which involve mainly the atomic displacements of the benzene ring[1] and give rise to a strong Raman band in resonance with the B_b transition, their Raman intensities are sensitive to environments, while their frequencies are insensitive. In contrast, for the W17 mode which involves atomic displacements of the pyrrole ring in addition to those of the benzene ring, its Raman intensity is weak but its frequency is sensitive to hydrogen bonding due to the involved vibrational movements of the N_1H group. As demonstrated in Figure 2, CD spectra of β15Trp and β37Trp were distinct. β15Trp yielded no fine structures, but β37Trp yielded vibronic bands at 279 nm (0 + 2172 cm^{-1}), 287 nm (0 + 1173 cm^{-1}), and 297 nm (0−0). Furthermore, in their CD spectra, β15Trp exhibited little difference between the T and R quaternary structures but β37Trp did exhibit an appreciable difference, weakening of the 0−1 and 0−2 transitions compared with the same 0−0 transitions. In accord with this, UVRR spectra of β15Trp yielded little difference between the T and R structures, whereas β37Trp exhibited a distinct intensity change, particularly for the W16, W17, and W18 bands. X-ray crystallographic analysis revealed little structural difference between the T and R structures for β15Trp but an appreciable difference in the hydrogen bonding conditions for β37Trp.[36]

Therefore, it is highly likely that the appearance of vibronic coupling in type-I CD spectra depends on the environment around the indole ring, particularly on hydrogen bonding under a hydrophobic environment. Presumably, W16 (1011 cm^{-1}) or W17 (879 cm^{-1}) vibrations contribute to the coupling with the L_b electronic transition. W17 is more likely because it involves vibrations of the pyrrole N_1H group and makes the L_b transition dipole active, but W16 is localized to the benzene ring,[1] although the vibrational modes and frequencies in the electronic excited state are somewhat different from those of the electronic ground state.

The 229 nm excited UVRR spectra observed for both L-Trp derivatives and indole-C_3 derivatives are alike and hardly influenced by different C_3 side chains except for W7, W9, and W10 bands. Kim and co-workers pointed out that the relative intensities of W10 (~1237 cm^{-1}) to W9 (~1254 cm^{-1}) in addition to the W7 doublet are sensitive to indole N_1H hydrogen bonding.[32] In fact, the N_1H hydrogen bond is sensitive to the C_3 side chain presumably due to steric hindrance. In contrast, no CD spectra were observed in the near-UV region for all indole-C_3 derivatives except for L-Trp. Moreover, CD spectra of L-Trp derivatives changed greatly by the modification of the amino group but much less by esterification of the carboxyl group.

The CD spectrum of L-Trp and L-Trp derivatives derived mainly from the L_a band is classified into type II, and that from the L_b band is classified into type I.[17] We point out here that CD of L-Trp derivatives becomes type II when its amino group is free but becomes type I when it is modified as in Nac-L-Trp EE and Nac-L-Trp. Edelhoch and Lippoldt[37] deduced from the experiments with three peptides, L-Trp-L-Tyr, L-Trp-L-Trp, and L-Tyr-L-Trp, that the 273 nm CD band (L_a) assignable to type II is stronger when L-Trp occupies the N-terminus than inside of proteins. These facts suggest that a modification of the amino group of L-Trp decreases optical activity in the L_a transition.[37]

Near-UV CD Spectra of Trp Residues in Proteins. The near-UV CD is usually used to monitor the tertiary and quaternary structures of proteins. Such CD bands derive mainly from Tyr and Trp residues that are interacting in an asymmetric environment.[17] In fact, CD spectra of individual Trp residues in proteins were extracted using mutation of each Trp residue;[12,38−40] four Trp residues in the extracellular domain of human tissue factor,[38] three Trp residues in pore-forming toxin (perfringolysin O) of *Clostridium perfringens* type A,[39] a single Trp residue in tear lipocalin,[40] and three Trp residues in human hemoglobin.[12] Although some of these CD bands were negative and some were positive, all of these CD spectra were of type I (L_b). In Hb A, α14- and β15Trp exhibited negative CD bands at 286 and 283 nm,[12] whereas β37Trp showed positive CD bands at 279 and 287 nm, as shown in Figure 2. Their differences were previously ascribed to the surrounding hydrophobicity on the basis of the solvent dependent spectral changes of Nac-L-Trp EE,[12] which displayed negative CD bands in hydrophobic solvents such as chloroform and CCl_4 but positive CD bands in hydrophilic solvent (water, methanol). Apparent CD spectra of type I seem to vary with the strength of vibronic coupling. For example, all the CD spectra in Figure 2 are grouped into type I on the basis of the peak positions; however, sometimes the spectrum shows strong vibronic features like β37Trp but sometimes very weak ones like β15Trp. Additionally, the features displayed quaternary structure dependence, that is, dependence on the surrounding hydrophobicity and hydrogen bonding.

dx.doi.org/10.1021/jp404685x | J. Phys. Chem. B 2013, 117, 9343−9353

The W17 frequencies of β15Trp and β37Trp revealed by UVRR spectra shown in Figure 3 indicate that both have hydrogen bonds and their strengths are hardly altered by the quaternary structure transitions. X-ray crystallographic analysis also demonstrated the presence of the N_1−H···O hydrogen bond between β15Trp and β72Ser and between β37Trp and α94Asp in deoxyHb A with T structure.[36] The hydrogen bond of β15Trp is retained similarly in the R structure, while that of β37Trp is kept but its partner is changed from α94Asp to β102Asn.[36] Thus, the difference between β15Trp and β37Trp in their CD spectra shown in Figure 2 may reflect relatively hydrophobic (β15Trp) or hydrophilic (β37Trp) environments, where a reformation of hydrogen bond does not occur or occurs, respectively, while Raman W17 frequencies indicated simply the presence of a hydrogen bond with similar strength in both T and R structures.

UVRR Spectra of L-Trp Residues and Indole-3 Derivatives. The 229 nm excited UVRR spectra as well as UV absorption spectra of L-Trp and Nac-L-Trp EE are almost the same (Figure 5), whereas their CD spectra are greatly different (Figure 4). This suggests that acetylation of the amino group hardly influences the π electronic structure of indole. Since the CD intensity depends on a product of electric transition-dipole and magnetic transition-dipole,[17] presumably acetylation of the amino group alters only the magnetic transition-dipole of indole through asymmetric C_α carbon.

Although the W7 band exhibits little difference between L-Trp and Nac-L-Trp EE (Figure 5), it exhibits appreciable changes with C_3 side chains of indole (Figure 6). Dieng and Schelvis[41] explained that the W7 doublet is caused by Fermi resonance between an in-plane fundamental mode around 1345 cm^{-1} and one or more out-of-plane (OOP) combination modes, 920 + 420 or 745 + 600 cm^{-1}.[41] Since the OOP modes are sensitive to an OOP distortion, the W7 doublet is thought to be sensitive to the environment around the indole ring. Accordingly, it is suggested that acetylation of the amino group hardly changes these OOP modes but C_3 substituents of indole do it. Indeed, C_3-methyl indole gives W7 as a singlet, presumably due to a shift of OOP modes,[32] although it was once interpreted as too small splitting.[29] The relative intensity of the W7 doublet of indole-C_3-acetic acid is different from that of L-Trp, and it is also caused by a shift of OOP modes.

Among indole derivatives shown in Figure 6, indole-C_3-pyruvic acid gave a high intensity for W1 relative to W3. W1 is considered to gain Raman intensity from the B_a electronic transition, while other modes such as W3, W7, and W16 gain intensity from the B_b electronic transition.[29] Therefore, the B_a electronic transition of indole-C_3-pyruvic acid, which corresponds to a far UV band around ∼195 nm, might be different from those of other indole-C_3 derivatives. Furthermore, only for indole-C_3-pyruvic acid, W2 band (1588 cm^{-1}) is observed, although W2 is reported to gain Raman intensity from the L_a electronic transition but not from B_a and B_b.[29] These features suggest that substitution of the C_3 side chain may affect characters of π electronic states of indole.

pH Dependent Changes of UVRR and CD Spectra of L-Trp. Figure 10 demonstrated that UVRR spectra of L-Trp are sensitive to deprotonation of both −COOH and $-NH_3^+$ groups, and these spectral changes are more prominent than those caused by acetylation of the amino group or esterification of the carboxyl groups. This suggests that an electric charge at both sides of C_α influences electronic states, especially the B_b electronic transition of indole. Deprotonation of amino and carboxyl groups commonly resulted in an appreciable increase in intensities of all RR bands except for the following features; deprotonation of the carboxyl group caused appearance of the 767 cm^{-1} component of W18, but that of the amino group decreased the intensity of W1 and the ∼1340 cm^{-1} component of W7. Although the shift of the W10 band to a lower wavenumber is caused by deprotonations of both carboxyl and amino groups, their amounts are somewhat different from each other; a shift due to a carboxyl group (1−2 cm^{-1}, see Figures SI1, SI2, and SI3, Supporting Information) is smaller than that due to an amino group (3−5 cm^{-1}, see Figures SI2, SI3, and SI4, Supporting Information). These observations may suggest that the π electronic state of indole is influenced by inductive effects through σ bonding: C_3(indole)−$C_\beta H_2$−C_αH−(NH_2 or COOH), and as a result, the presence of negatively charged carboxyl (−COO^-) and positively charged amino ($-NH_3^+$) groups perturbs the π electronic state more sensitively than esterification of the carboxyl group or acetylation of amino groups. The difference between the effects of deprotonation of amino and carboxyl groups may reflect the differences between the amounts of electric charges on nitrogen of $-NH_3^+$ and on carbon of −COOH, which are directly bound to C_α. In other words, deprotonation of a carboxyl group changes the charge density of an oxygen atom but not that of a carbon atom.

Anyways, it is noted that these intensity changes upon deprotonation are phenomenologically very similar to those observed when HMPA (hexamethylphosphoric triamide) was added to Nac-L-Trp EE in CCl_4. HMPA is known to serve as a strong hydrogen bond acceptor[29,32] and to interact with N_1H of the indole ring.[12] In this case, indole serves as a proton donor of the hydrogen bond, and therefore, would be slightly negative-charged. However, it occurs in hydrophobic solvents and, therefore, its mechanism would be presumably different from that for deprotonation, because the latter takes place in a hydrophilic environment.

For CD spectra of L-Trp derivatives, on the other hand, we have previously pointed out that Nac-L-Trp EE in hydrophobic solvents gives two CD bands at 284 nm (0 + 847 cm^{-1}) and 291 nm (0−0) and the addition of HMPA caused an intensity decrease of the former and increase of the latter with a shift to 293 nm.[12] This feature suggested the vibronic features are related to the N_1H hydrogen bonding. However, pH dependent changes of Nac-L-Trp do not show such features in Figure 9, suggesting that the pH changes hardly affect the N_1H hydrogen bond. This is consistent with the fact that the Raman hydrogen-bond marker (W17) did not show pH dependent frequency shift. The pH invariance of frequency separations in vibronic coupling of Nac-L-Trp in Figure 9 is also consistent with it. Therefore, the changes of CD spectra by pH arise through the σ bonding system of C_3−C_β−C_α−COO^- (or $-NH_3^+$) but not through the N_1H hydrogen bond of indole. The relative strength of L_a and L_b CD bands may also depend on the same factor.

Increases of positive intensity in CD spectra of L-Trp derivatives at acidic pH (Figure 9) apparently resemble the increases in positive intensity of CD bands of Trpβ37 of Hb A upon the T to R transition (Figure 2).[12] The pI values of deoxy Hb A (7.10) and COHb (6.95)[42] mean that a charge of COHb is more negative (or less positive) than that of deoxyHb at neutral pH (7.40), and therefore cannot interpret the behavior of Trpβ37. On the other hand, considering that pK_a values of several His residues are higher for oxyHb A (R state) than for deoxyHb A (T state),[43−45] the general atmosphere within

dx.doi.org/10.1021/jp404685x | J. Phys. Chem. B 2013, 117, 9343−9353

globin is more negative in the R than T quaternary structures at pH 7.4. This is also against the expected increase of positive charge. Therefore, the increases of positive intensity of CD bands for Trpβ37 of Hb A upon the T to R transition would be due to a decrease in surrounding hydrophobicity.[12]

In conclusion, it became clear that UVRR and CD spectra of L-Trp derivatives are changed by electric charges on both sides of C_α. When Trp derivatives are placed in a hydrophilic environment with less negative surrounding charges, the positive CD band is more intense but the W3, W7 (~1360 cm^{-1}), W16, W17, and W18 bands in UVRR become weaker. In Hb A, Trpβ37 yields a more intense positive CD band and less intense W3, W7 (~1360 cm^{-1}), W16, W17, and W18 bands in UVRR in the R than T state. Thus, the present study demonstrated that CD and UVRR spectra of L-Trp derivatives are sensitive to subtle changes in surrounding electric charges.

■ ASSOCIATED CONTENT

Supporting Information

Detailed UVRR spectra and pH dependences of model compounds. The absorption spectrum of L-Trp in water and the transition dipole moments of L_a, L_b, and B_b bands. This material is available free of charge via the Internet at http://pubs.acs.org.

■ AUTHOR INFORMATION

Corresponding Author

*E-mail: nagatomo@chem.tsukuba.ac.jp (S.N.); teizo@sci.u-hyogo.ac.jp (T.K.).

Notes

The authors declare no competing financial interest.

■ ACKNOWLEDGMENTS

We thank Professor Chien Ho of Carnegie Mellon University for the gift of the *E. coli* Hb expression plasmid, pHE7, and Dr. Yayoi Aki of Kanazawa University for construction plasmids and expressing mutant Hb's. This study was supported by a Grant-in-Aid from the Ministry of Education, Culture, Sports, Science, and Technology for Scientific Research (B) to T.K. (24350086).

■ ABBREVIATIONS

Hb A, human adult hemoglobin; Trp, tryptophan; L-Trp ME, L-tryptophan methylester; Nac-L-Trp, *N*-acetyl-L-tryptophan; Nac-L-Trp EE, *N*-acetyl-L-tryptophan ethylester; CD, circular dichroism; UVRR, ultraviolet resonance Raman

■ REFERENCES

(1) Harada, I.; Takeuchi, H. *Raman and Ultraviolet Resonance Raman Spectra of Proteins and Related Compounds, Spectroscopy of Biological Systems*; Clark, R. J. H., Hester, R. E., Eds.; John Wiley & Sons Ltd: New York, 1986; Vol. *13*, Chapter 3.

(2) Rodgers, K. R.; Su, C.; Subramaniam, S.; Spiro, T. G. Hemoglobin R→T Structural Dynamics from Simultaneous Monitoring of Tyrosine and Tryptophan Time-Resolved UV Resonance Raman Signals. *J. Am. Chem. Soc.* **1992**, *114*, 3697−3709.

(3) Cho, N.; Song, S.; Asher, S. A. UV Resonance Raman and Excited-State Relaxation Rate Studies of Hemoglobin. *Biochemistry* **1994**, *33*, 5932−5941.

(4) Nagai, M.; Kaminaka, S.; Ohba, Y.; Nagai, Y.; Mizutani, Y.; Kitagawa, T. Ultraviolet Resonance Raman Studies of Quaternary Structure of Hemoglobin Using a Tryptophan β37 Mutant. *J. Biol. Chem.* **1995**, *270*, 1636−1642.

(5) Hu, X.; Spiro, T. G. Tyrosine and Tryptophan Structure Markers in Hemoglobin Ultraviolet Resonance Raman Spectra: Mode Assignments via Subunit-Specific Isotope Labeling of Recombinant Protein. *Biochemistry* **1997**, *36*, 15701−15712.

(6) Kiger, L.; Klinger, A. L.; Kwiatkowski, L. D.; De Young, A.; Doyle, M. L.; Holt, J. M.; Noble, R. W.; Ackers, G. K. Thermodynamic Studies on the Equilibrium Properties of a Series of Recombinant βW37 Hemoglobin Mutants. *Biochemistry* **1998**, *37*, 4336−4345.

(7) Nagatomo, S.; Jin, Y.; Nagai, M.; Hori, H.; Kitagawa, T. Changes in the Abnormal α-Subunit upon CO-Binding to the Normal β-Subunit of Hb M Boston: Resonance Raman, EPR, and CD Study. *Biophys. Chem.* **2002**, *98*, 217−232.

(8) Samuni, U.; Juszczak, L.; Dantsker, D.; Khan, I.; Friedman, A. J.; Perez-Gonzalez-de-Apodaca, J.; Bruno, S.; Hui, H. L.; Golby, J. E.; et al. Functional and Spectroscopic Characterization of Half-Liganded Iron-Zinc Hybrid Hemoglobin: Evidence for Conformational Plasticity within the T State. *Biochemistry* **2003**, *42*, 8272−8288.

(9) Nagatomo, S.; Nagai, M.; Mizutani, Y.; Yonetani, T.; Kitagawa, T. Quaternary Structures of Intermediately Ligated Human Hemoglobin A and Influences from Strong Allosteric Effectors: Resonance Raman Investigation. *Biophys. J.* **2005**, *89*, 1203−1213.

(10) Samuni, U.; Roche, C. J.; Dantsker, D.; Juszczak, L. J.; Friedman, J. M. Modulation of Reactivity and Conformation within the T-Quaternary States of Human Hemoglobin: The Combined Use of Mutagenesis and Sol-Gel Encapsulation. *Biochemistry* **2006**, *45*, 2820−2835.

(11) Nagatomo, S.; Nagai, M.; Kitagawa, T. In *Hemoglobin: Recent Developments and Topics*; Nagai, M., Ed.; Research Signpost: Kerala, India, 2011; Chapter 3, pp 37−61.

(12) Nagai, M.; Nagatomo, S.; Nagai, Y.; Ohkubo, K.; Imai, K.; Kitagawa, T. Near-UV Circular Dichroism and UV Resonance Raman Spectra of Individual Tryptophan Residues in Human Hemoglobin and Their Changes upon the Quaternary Structure Transition. *Biochemistry* **2012**, *51*, 5932−5941.

(13) Simon, S. R.; Cantor, C. R. Measurement of Ligand-Induced Conformational Changes in Hemoglobin by Circular Dichroism. *Proc. Natl. Acad. Sci. U.S.A.* **1969**, *63*, 205−212.

(14) Perutz, M. F.; Ladner, J. E.; Simon, S. R.; Ho, C. Influence of Globin Structure on the State of the Heme. I. Human Deoxyhemoglobin. *Biochemistry* **1974**, *13*, 2163−2173.

(15) Jin, Y.; Sakurai, H.; Nagai, Y.; Nagai, M. Changes of Near-UV CD Spectrum of Human Hemoglobin upon Oxygen Binding: A Study of Mutants at α42, α140, β145 Tyrosine or β37 Tryptophan. *Biopolymers* **2004**, *74*, 60−63.

(16) Aki-Jin, Y.; Nagai, Y.; Imai, K.; Nagai, M. Changes of Near-UV Circular Dichroism Spectra of Human Hemoglobin upon the R → T Quaternary Structure Transition. In *New Approarches in Biomedical Spectroscopy*; ACS Symposium Series 963; Kneipp, K., Aroca, R., Kneipp, H., Wentrup-Byrne, E., Eds.; American Chemical Society: Washington, DC, 2007; pp 297−311.

(17) Strickland, E. H. Aromatic Contributions to Circular Dichroism Spectra of Proteins. *CRC Crit. Rev. Biochem.* **1974**, *2*, 113−175.

(18) Shen, T. J.; Ho, N. T.; Zou, M.; Sun, D. P.; Cottam, P. F.; Simplaceanu, V.; Tam, M. F.; Bell, D. A., Jr.; Ho, C. Production of Human Normal Adult and Fetal Hemoglobins in *Escherichia coli*. *Protein Eng.* **1997**, *10*, 1085−1097.

(19) Chen, Z.; Ruffner, D. E. Amplification of Closed Circular DNA *in vitro*. *Nucleic Acids Res.* **1998**, *26*, 1126−1127.

(20) Nagai, M.; Nagai, Y.; Aki, Y.; Imai, K.; Wada, Y.; Nagatomo, S.; Yamamoto, Y. Effect of Reversed Heme Orientation on Circular Dichroism and Cooperative Oxygen Binding of Human Adult Hemoglobin. *Biochemistry* **2008**, *47*, 517−525.

(21) Kaminaka, S.; Kitagawa, T. A Novel Idea for Practical UV Resonance Raman Measurement with a Double-Monochromator and Its Application to Protein Structural Studies. *Appl. Spectrosc.* **1992**, *46*, 1804−1808.

(22) Kaminaka, S.; Kitagawa, T. Novel Spinning Cell System for UVRR Measurements of Powder and Small-Volume Solution Samples

in Back-Scattering Geometry: Application to Solid Tryptophan and Mutant Hemoglobin Solution. *Appl. Spectrosc.* **1995**, *49*, 685−687.
(23) Dudik, J. M.; Johnson, C. R.; Asher, S. A. Wavelength Dependence of the Preresonance Raman Cross Sections of CH_3CN, SO_4^{2-}, ClO_4^-, and NO_3^-. *J. Chem. Phys.* **1985**, *82*, 1732−1740.
(24) Harada, I.; Miura, T.; Takeuchi, H. Origin of the Doublet at 1360 cm^{-1} and 1340 cm^{-1} in the Raman Spectra of Tryptophan and Related Compounds. *Spectrochim. Acta, Part A* **1986**, *42*, 307−312.
(25) Miura, T.; Takeuchi, H.; Harada, I. Characterization of Individual Tryptophan Side Chains in Proteins Using Raman Spectroscopy and Hydrogen-Deuterium Exchange Kinetics. *Biochemistry* **1988**, *27*, 88−94.
(26) Miura, T.; Takeuchi, H.; Harada, I. Tryptophan Raman Bands Sensitive to Hydrogen Bonding and Side-Chain Conformation. *J. Raman Spectrosc.* **1989**, *20*, 667−671.
(27) Chi, Z.; Asher, S. A. UV Raman Determination of the Environment and Solvent Exposure of Tyr and Trp Residues. *J. Phys. Chem. B* **1998**, *102*, 9595−9602.
(28) Chi, Z.; Asher, S. A. Ultraviolet Resonance Raman Examination of Horse Apomyoglobin Acid Unfolding Intermediates. *Biochemistry* **1999**, *38*, 8196−8203.
(29) Matsuno, M.; Takeuchi, H. Effects of Hydrogen Bonding and Hydrophobic Interactions on the Ultraviolet Resonance Raman Intensities of Indole Ring Vibrations. *Bull. Chem. Soc. Jpn.* **1998**, *71*, 851−857.
(30) Strickland, E. H.; Horwitz, J.; Billups, C. Near-Ultraviolet Absorption Bands of Tryptophan. Studies Using Indole and 3-Methylindole as Models. *Biochemistry* **1970**, *9*, 4914−4921.
(31) Strickland, E. H.; Billups, C.; Kay, E. Effects of Hydrogen Bonding and Solvents upon the Tryptophanyl ^1L_a Absorption Band. Studies Using 2,3-Dimethylindole. *Biochemistry* **1972**, *11*, 3657−3662.
(32) Schlamadinger, D. E.; Gable, J. E.; Kim, J. E. Hydrogen Bonding and Solvent Polarity Markers in the UV Resonance Raman Spectrum of Tryptophan: Application to Membrane Proteins. *J. Phys. Chem. B* **2009**, *113*, 14769−14778.
(33) Albinsson, B.; Norden, B. Excited-State Properties of the Indole Chromophore. Electronic Transition Moment Directions from Linear Dichroism Measurements: Effect of Methyl and Methoxy Substituents. *J. Phys. Chem.* **1992**, *96*, 6024−6212.
(34) Valeur, B.; Weber, G. Resolution of the Fluorescence Excitation Spectrum of Indole into the ^1L_a and ^1L_b Excitation Bands. *Photochem. Photobiol.* **1977**, *25*, 441−444.
(35) Strickland, E. H.; Billups, C. Oscillator Strength of the ^1L_a and ^1L_b Absorption Bands of Tryptophan and Several Other Indoles. *Biopolymers* **1973**, *12*, 1989−1995.
(36) Park, S. Y.; Yokoyama, T.; Shibayama, N.; Shiro, Y.; Tame, J. R. H. 1.25 Å Resolution Crystal Structures of Human Haemoglobin in the Oxy, Deoxy and Carbonmonoxy Forms. *J. Mol. Biol.* **2006**, *360*, 690−701.
(37) Edelhoch, H.; Lippoldt, R. E. The Circular Dichroism of Tyrosyl and Tryptophanyl Diketopiperazines. *J. Biol. Chem.* **1968**, *243*, 4799−4805.
(38) Andersson, D.; Carlsson, U.; Freskgård, P. Contribution of Tryptophan Residues to the CD Spectrum of the Extracellular Domain of Human Tissue Factor. *Eur. J. Biochem.* **2001**, *268*, 1118−1128.
(39) Nakamura, M.; Sekino-Suzuki, N.; Mitsui, K.; Ohno-Iwashita, Y. Contribution of Tryptophan Residues to the Structural Changes in Perfringolysin O during Interaction with Liposomal Membaranes. *J. Biochem.* **1998**, *123*, 1145−1155.
(40) Gasymov, O. K.; Abduragimov, A. R.; Yusifov, T. N.; Glasgow, B. J. Resolving near-Ultraviolet Circular Dichroism Spectra of Single Trp Mutants in Tear Lipocalin. *Anal. Biochem.* **2003**, *318*, 300−308.
(41) Dieng, S. D.; Schelvis, J. P. M. Analysis of Measured and Calculated Raman Spectra of Indole, 3-Methylindole, and Tryptophan on the Basis of Observed and Predicted Isotope Shifts. *J. Phys. Chem. A* **2010**, *114*, 10897−10905.
(42) Bunn, H. F.; Forget, B. G. *Hemoglobin: Molecular, Genetic and Clinical Aspects*; Sounders Company: Philadelphia, PA, 1986; pp 663−675.
(43) Perutz, M. F. Stereochemistry of Cooperative Effects in Haemoglobin. *Nature* **1970**, *228*, 726−739.
(44) Kilmartin, J. V.; Breen, J. J.; Roberts, G. C. K.; Ho, C. Direct Measurement of the p*K* Values of an Alkaline Bohr Group in Human Hemoglobin. *Proc. Natl. Acad. Sci. U.S.A.* **1973**, *70*, 1246−1249.
(45) Ohe, M.; Kajita, A. Changes in pK_a Values of Individual Histidine Residues of Human Hemoglobin upon Reaction with Carbon Monoxide. *Biochemistry* **1980**, *19*, 4443−4450.